Implications of Sea Breeze Circulations on Boundary Layer Aerosols in the Southern Coastal Texas Region

Tamanna Subba[1], Michael P. Jensen[1], Min Deng[1], Scott E. Giangrande[1], Mark C. Harvey[2], Ashish Singh[1], Die Wang[1], Maria Zawadowicz[1], Chongai Kuang[1]

[1]Environmental Science and Technologies, Brookhaven National Laboratory, Upton, NY, United States

[2]Department of Physics, Texas Southern University, Houston, TX, United States

These figures are the supporting information for the manuscript.

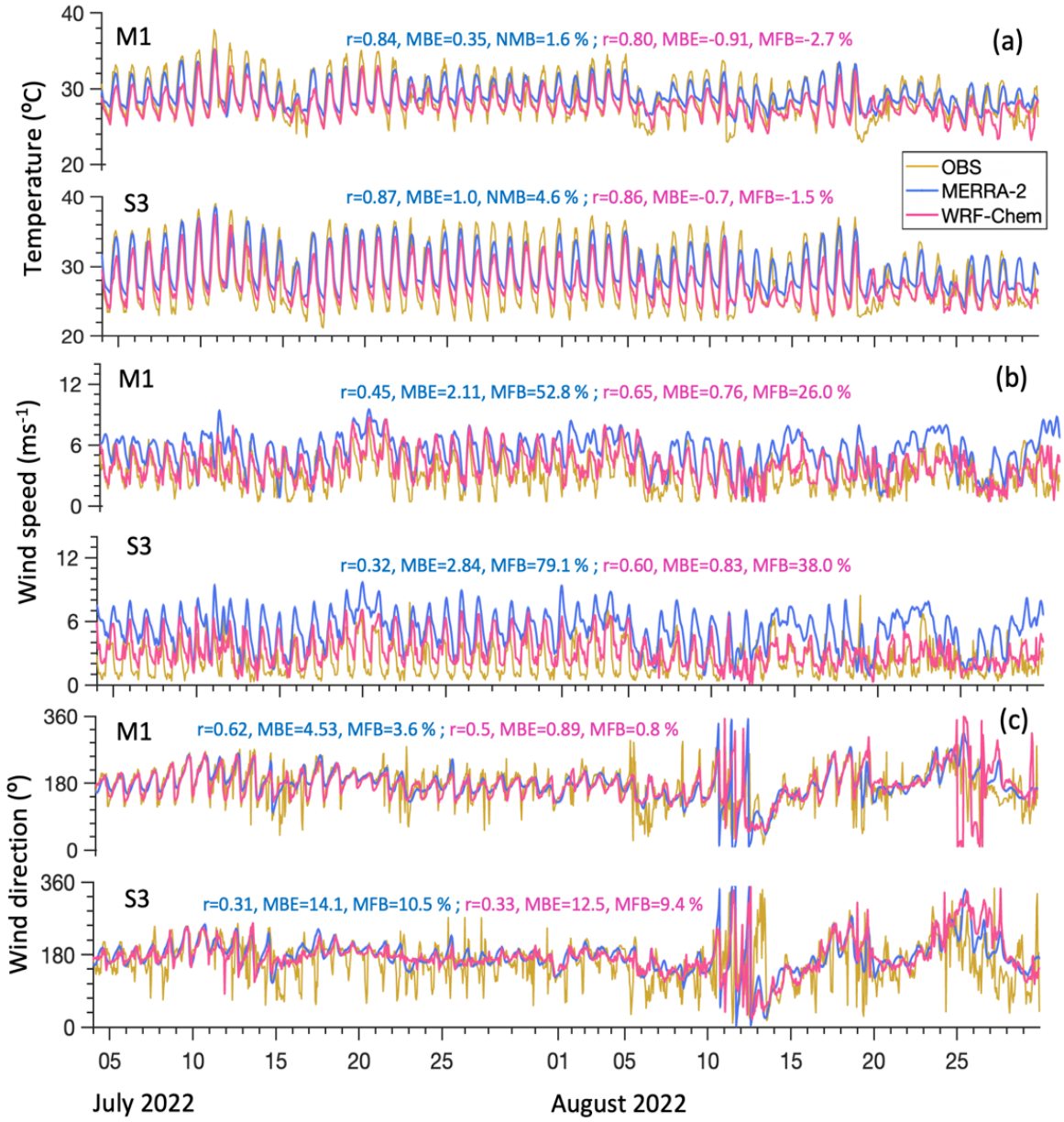

Figure S1. Time series of hourly meteorological variables (a) Temperature at 2 m, (b) wind speed at 10 m, and (c) wind direction at 10 m at M1 and S3 sites observed (yellow), WRF-Chem simulated (pink), and MERRA-2 retrieved (blue) from 04 July- 30 August 2022.

MERRA-2: Modern-Era Retrospective analysis for Research and Applications, Version 2 (Gelaro, R., and Coauthors: The Modern-Era Retrospective Analysis for Research and Applications, version 2 (MERRA-2). J. Climate, 30, 5419–5454, https://doi.org/10.1175/JCLI-D-16-0758.1, 2017.)

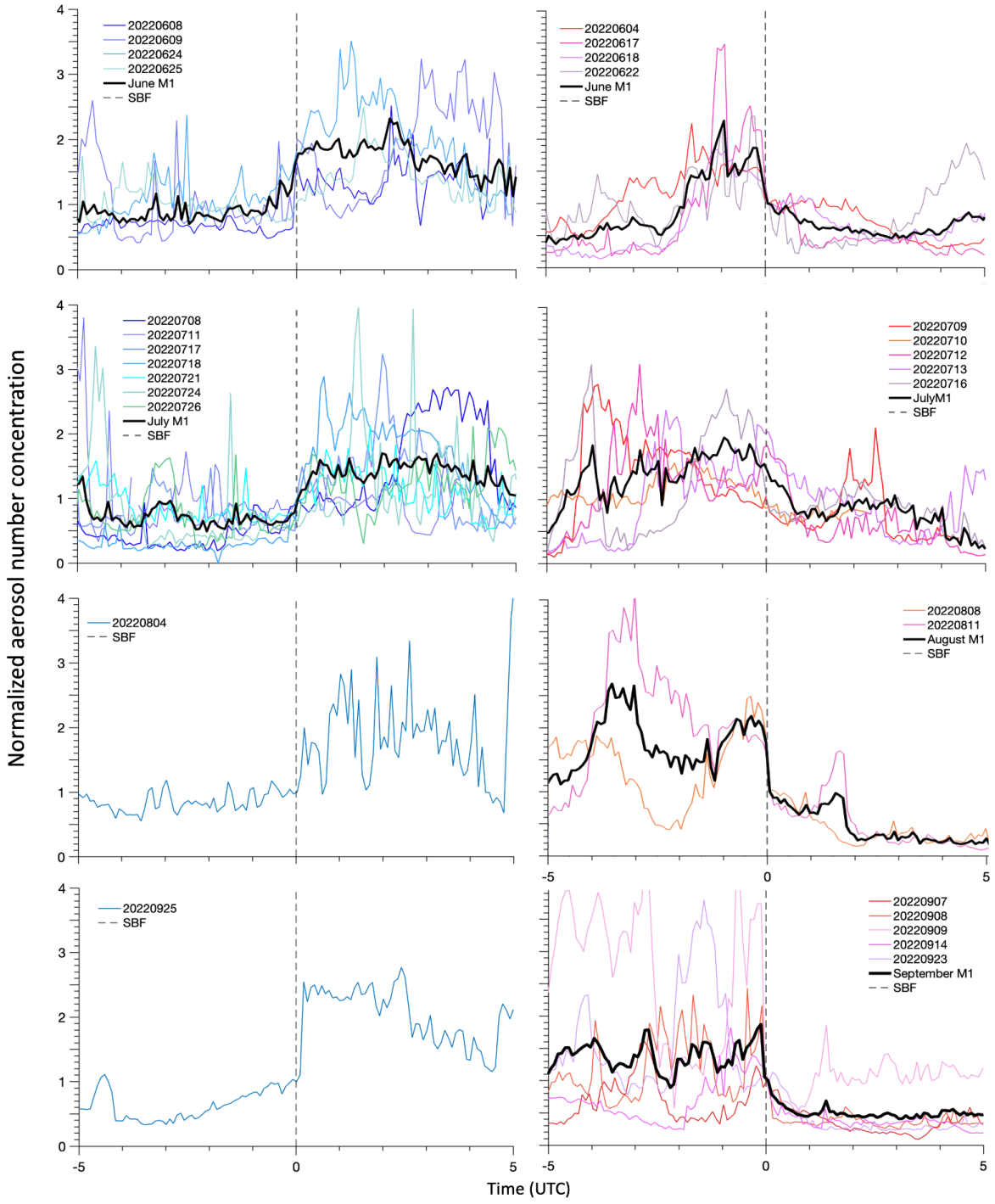

Figure S2. (a) Time series of the normalized aerosol number concentration, with time normalized w.r.t the time of the sea breeze front (SBF)'s passing through the M1 site during the individual SB event days.

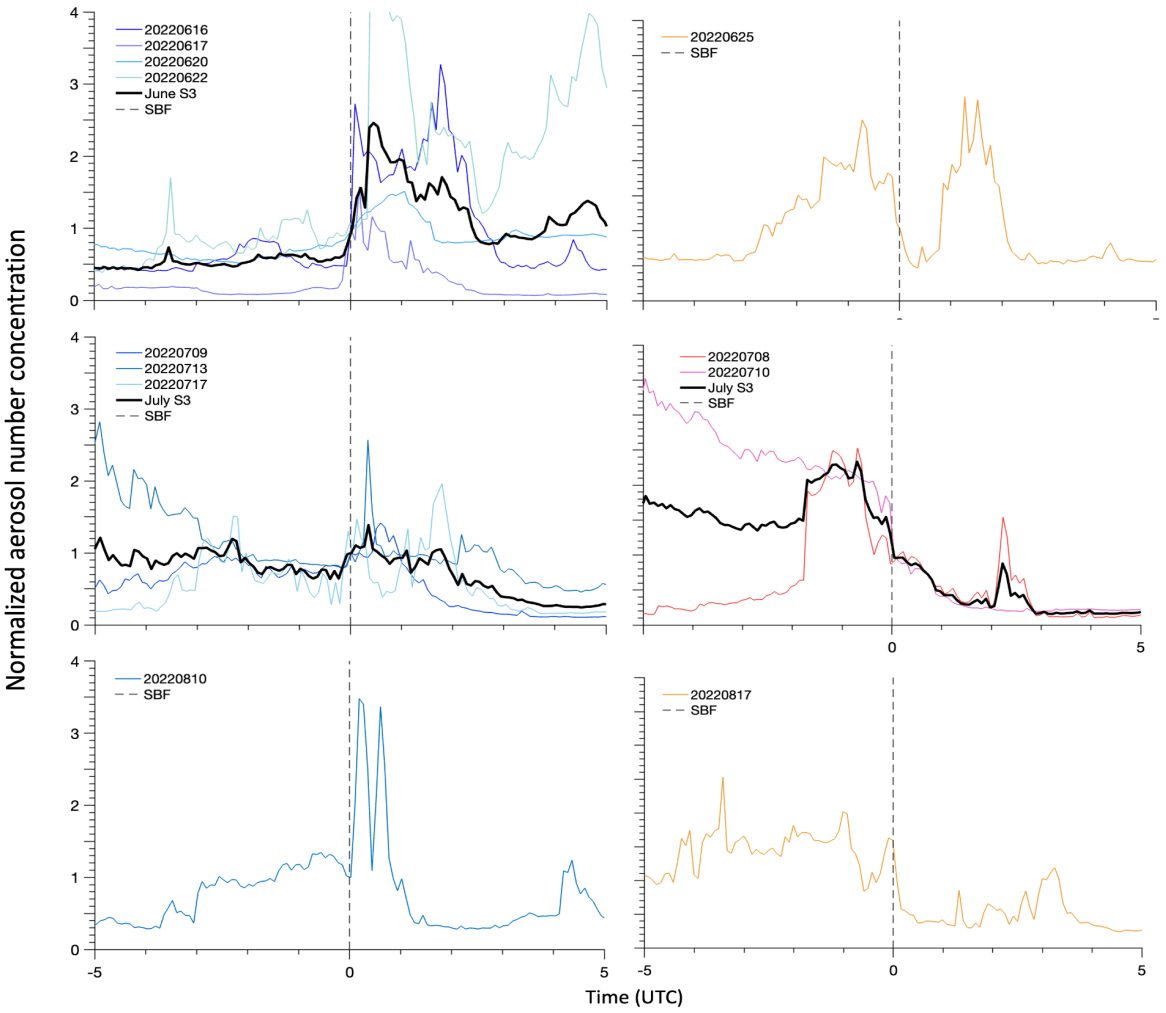

Figure S3. (a) Time series of the normalized aerosol number concentration, with time normalized w.r.t the time of the sea breeze front (SBF)'s passing through the S3 site during the individual SB event days.

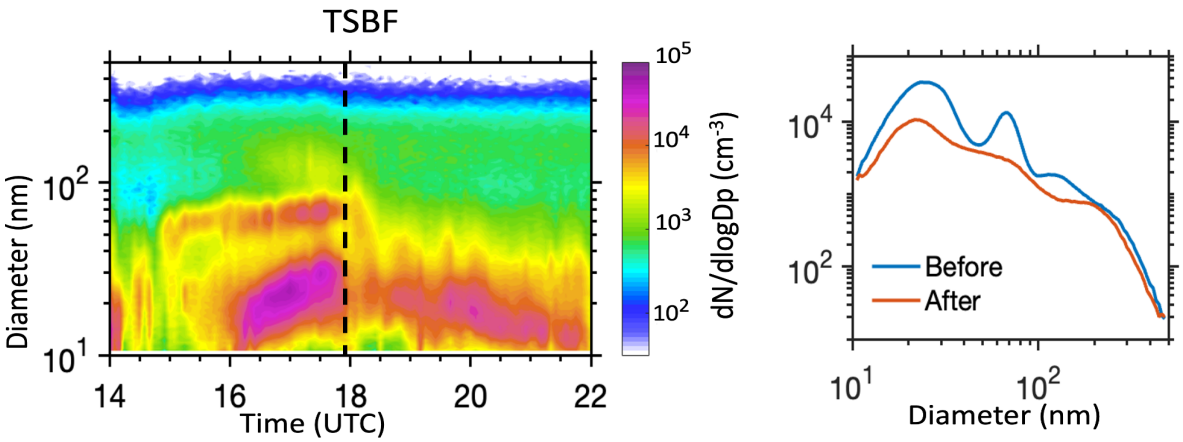

Figure S4. Time series of measured aerosol size distribution at the M1 site on 16 July. The black dashed line represents the time of the passing of the SBF (T_{SBF}).

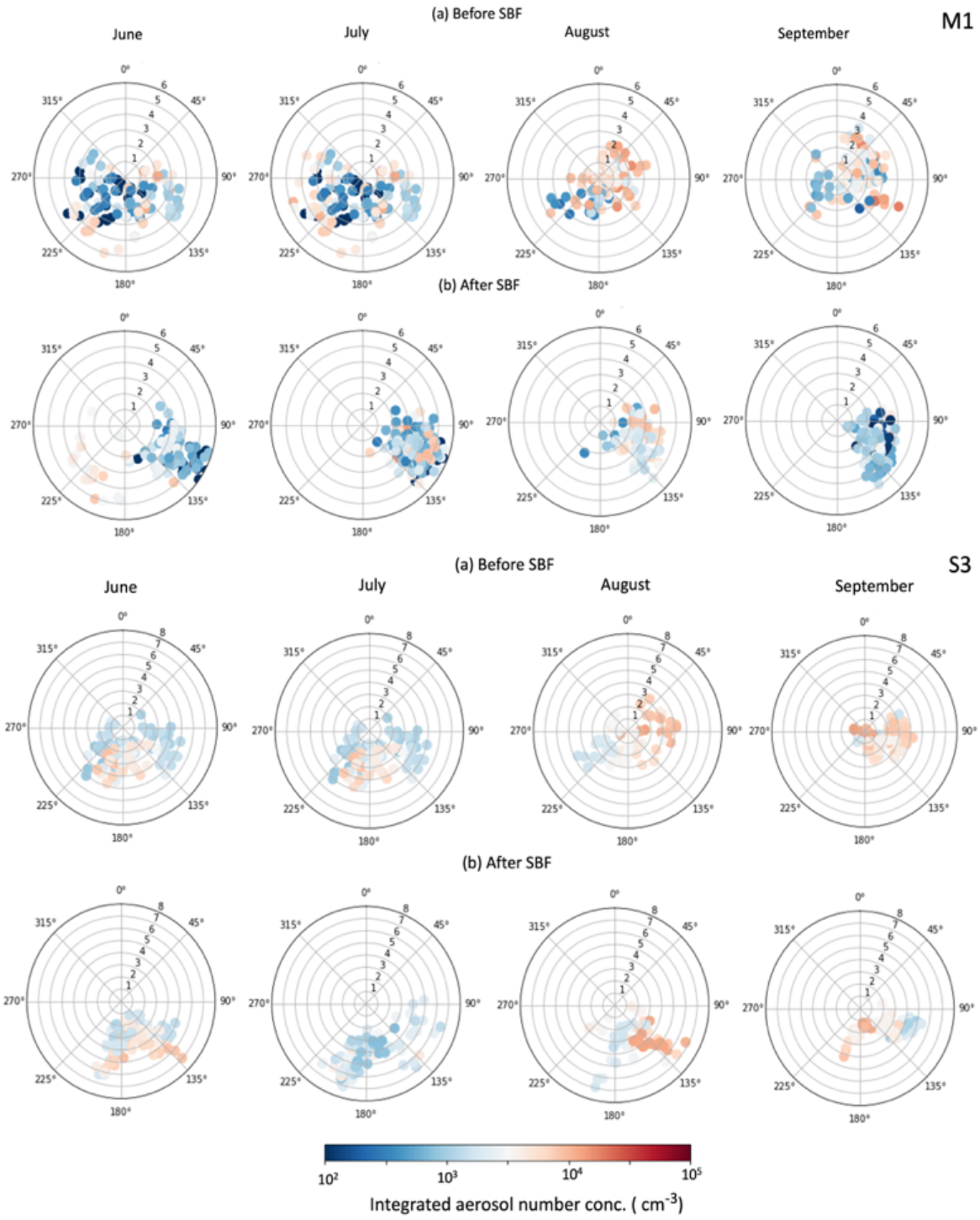

Figure S5. Open-air polar plots for integrated aerosol number concentration before and after the passing of the sea breeze front at M1 and S3 sites during June to September 2022. The wind speed (in m s^{-1}) grid lines are presented with black circles. The color scales represent the concentrations observed with each wind speed and direction combinations.

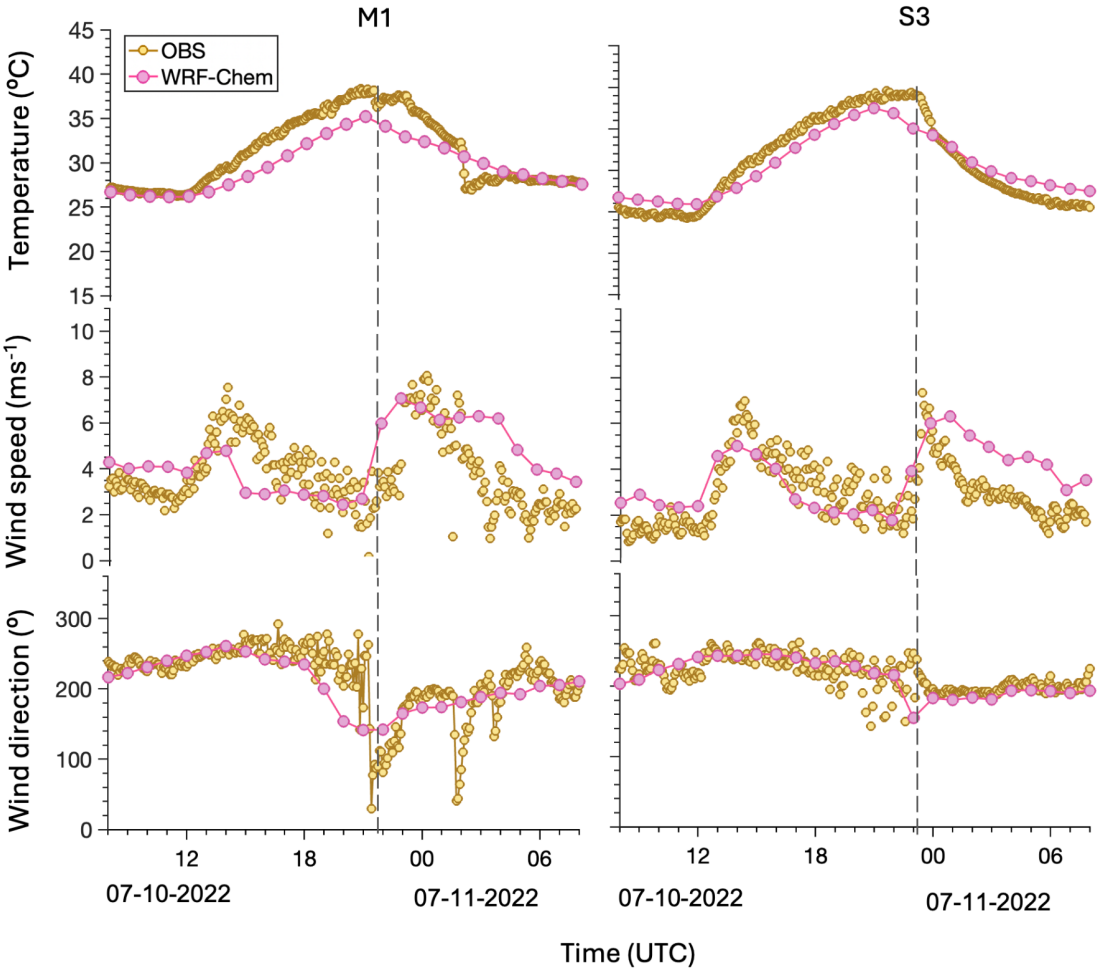

Figure S6. Time series of temperature, wind speed, and wind directions measured and modeled at M1 and S3 sites.

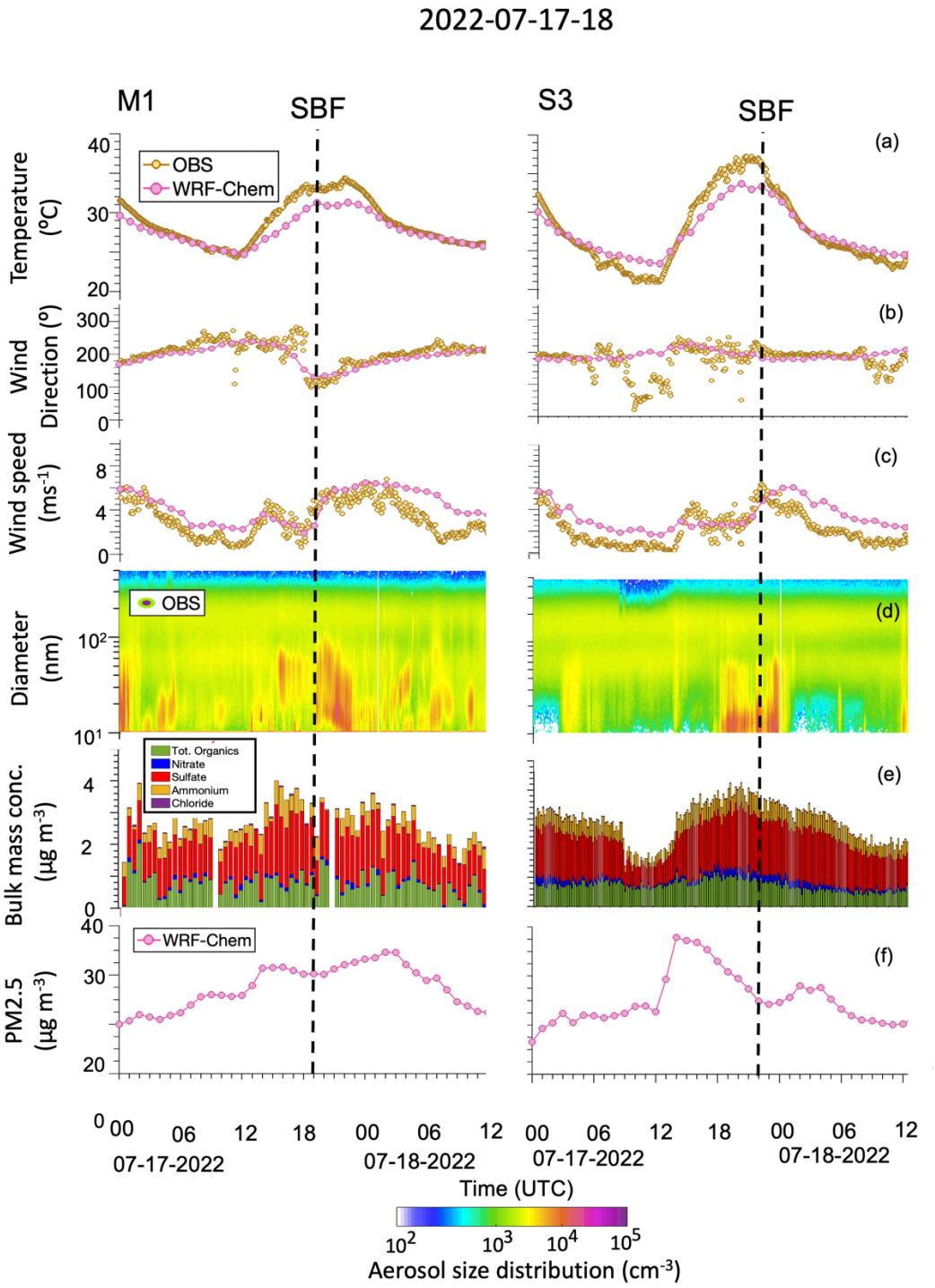

Figure S7. Time series of measured and modeled (a) temperature, (b) wind directions, (c) wind speed, (d) measured aerosol size distribution, (e) measured bulk chemical composition, and (f) modeled $PM_{2.5}$. The black dashed line represents the time of the passing of the SBF (T_{SBF}) at the respective sites.

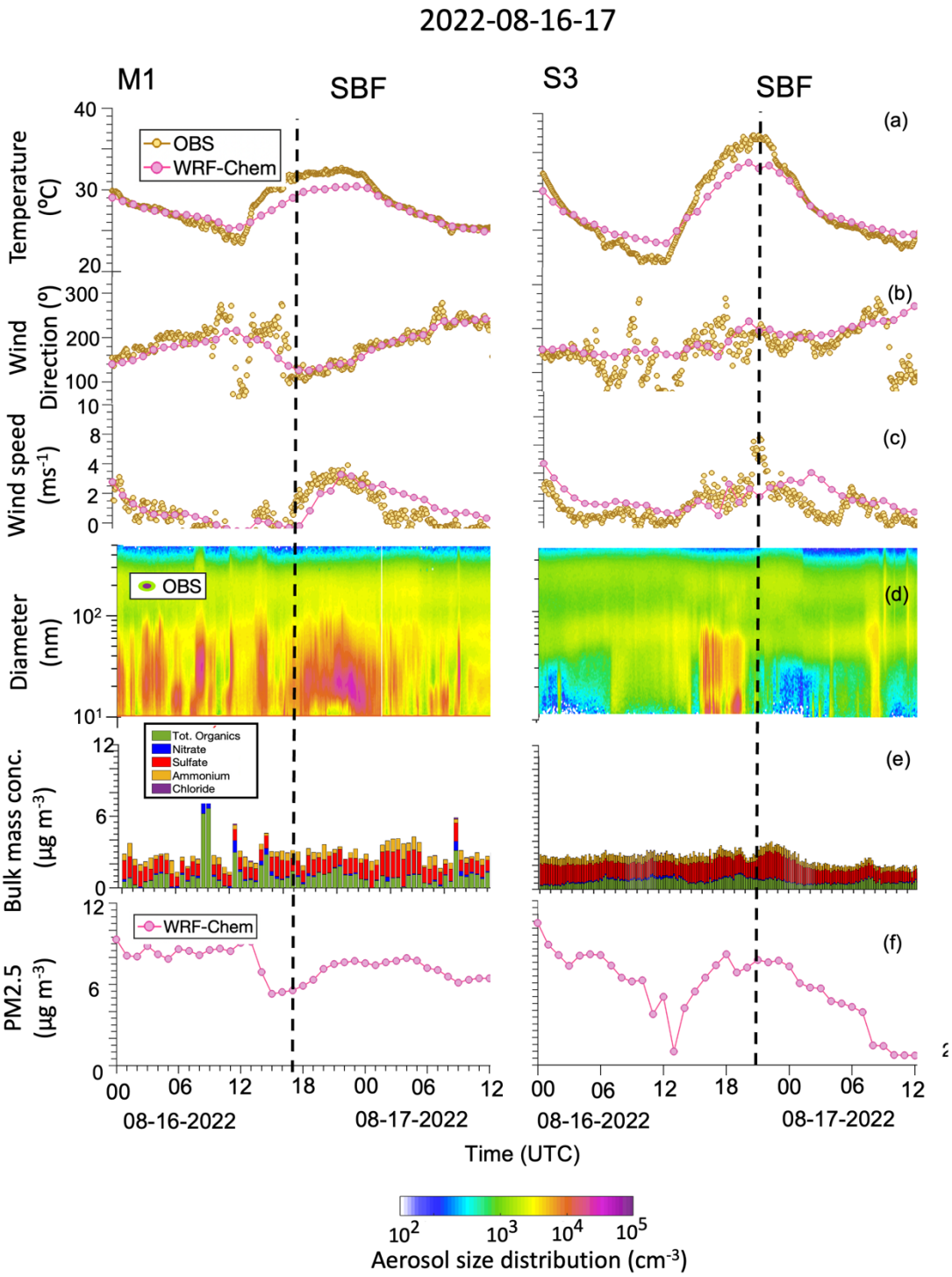

Figure S8. Time series of measured and modeled (a) temperature, (b) wind directions, (c) wind speed, (d) measured aerosol size distribution, (e) measured bulk chemical composition, and (f) modeled $PM_{2.5}$. The black dashed line represents the time of the passing of the SBF (T_{SBF}) at the respective sites.

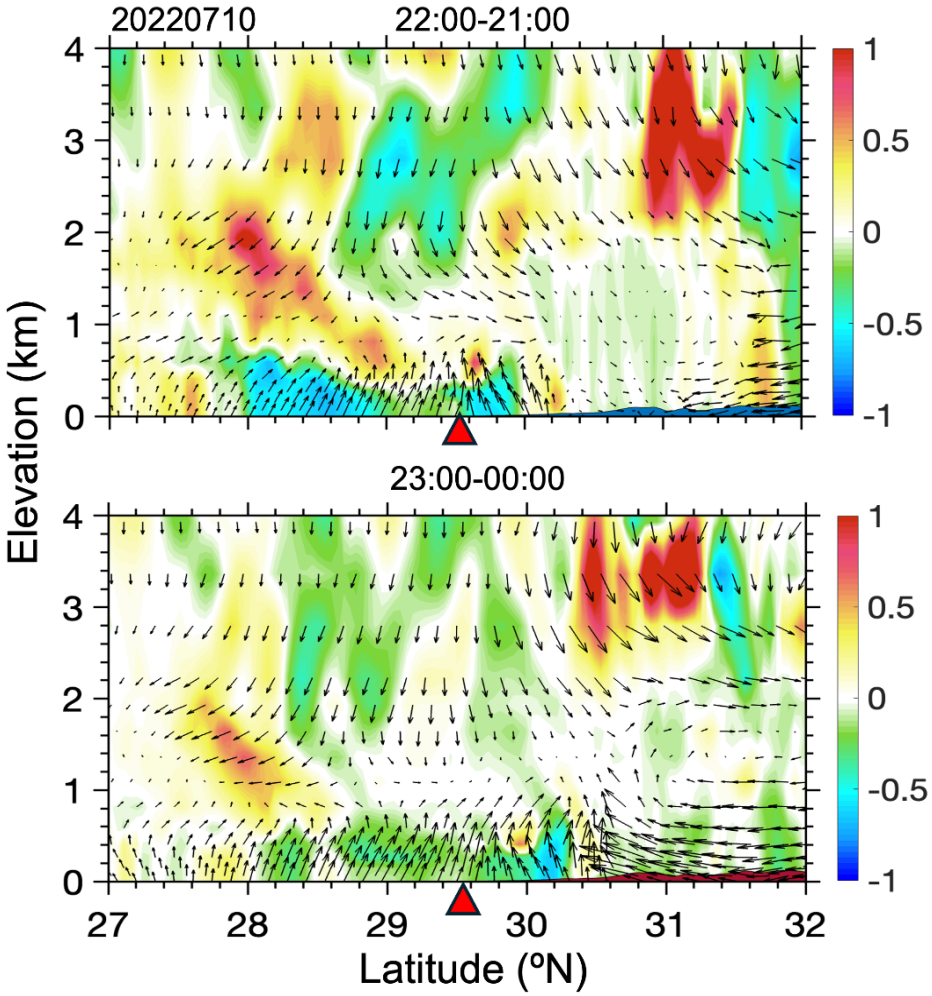

Figure S9. Vertical distribution of WRF-Chem simulated $PM_{2.5}$ on sea-breeze day 10 July 2022 (SBF time is 21:30 UTC). (a) The $PM_{2.5}$ bias between two time steps along the latitudes across the M1 site (marked by the red triangle).

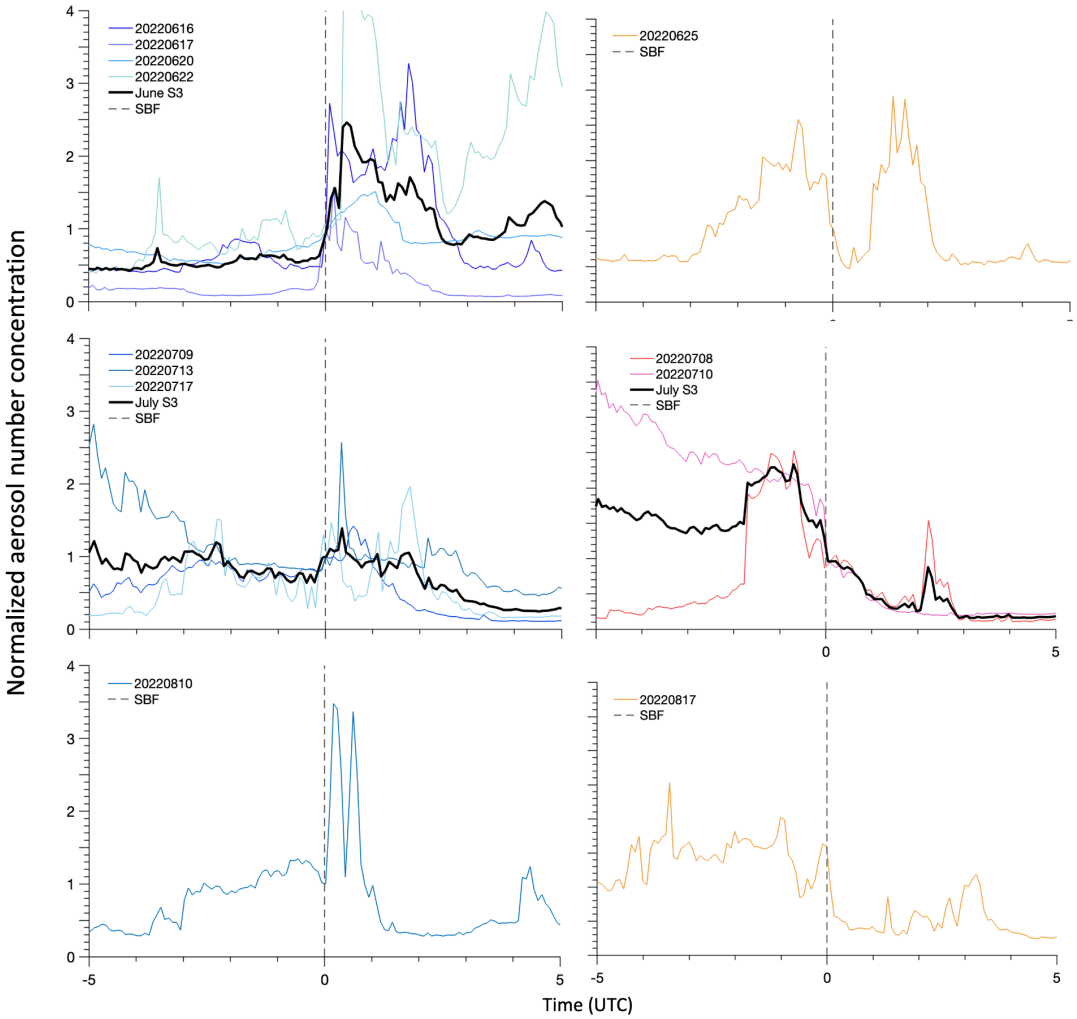

Figure S10. Time series of the normalized N100, with time normalized w.r.t the time of the sea breeze front (SBF)'s passing through the M1 site during the individual SB event days.

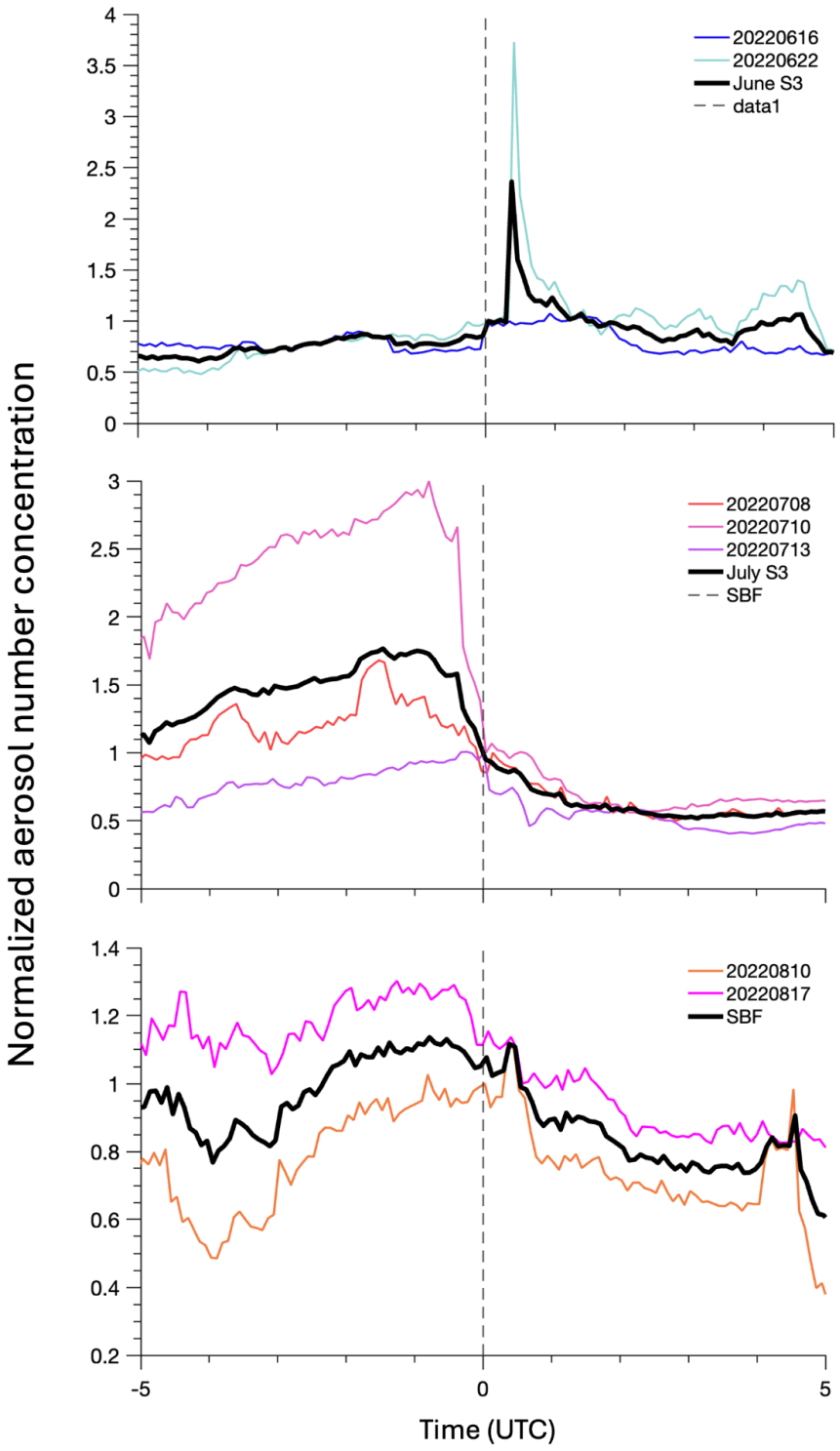

Figure S11. Time series of the normalized N100, with time normalized w.r.t the time of the sea breeze front (SBF)'s passing through the S3 site during the individual SB event days.

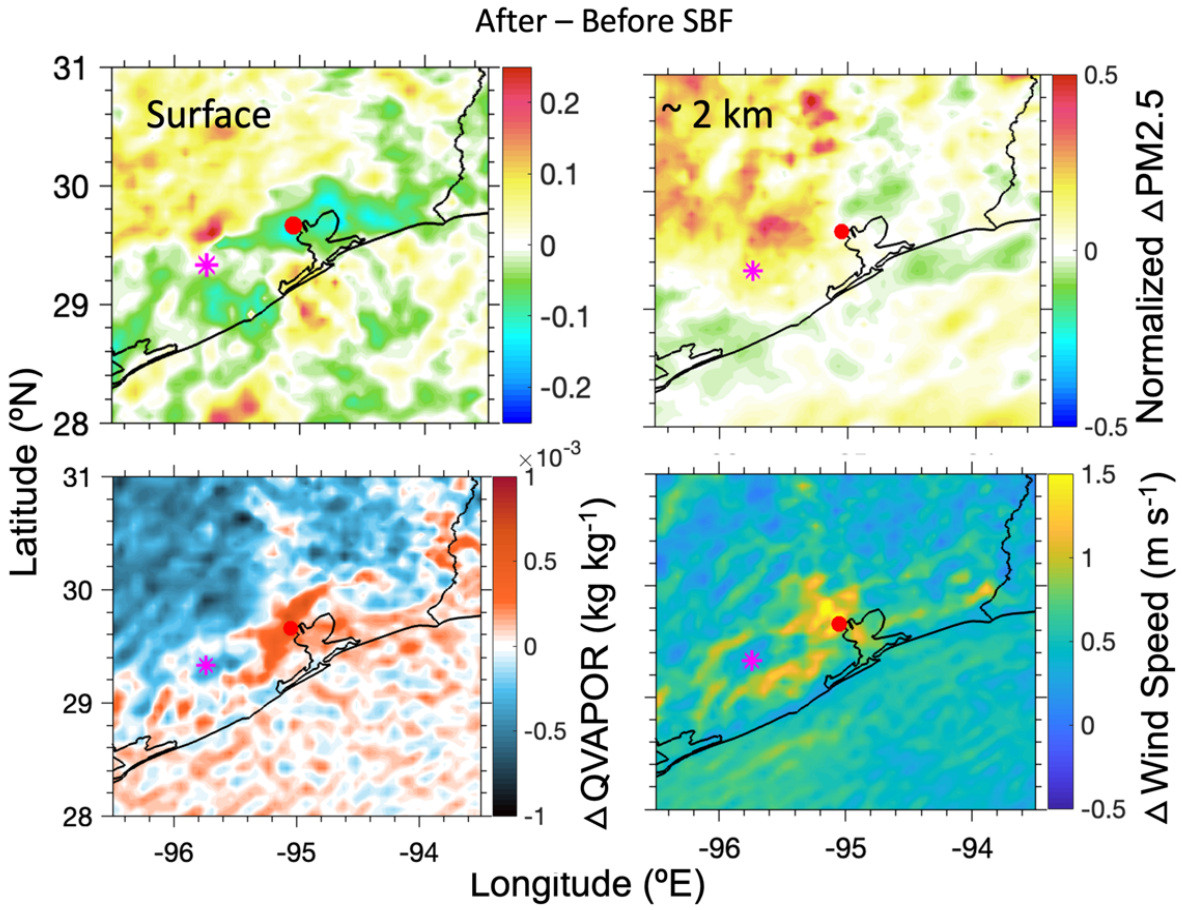

Figure S12. Modeled difference of $PM_{2.5}$ concentrations at the surface, at 2km, water vapor mixing ratio, and wind speed averaged over 18 sea breeze days before and after the passing of the SBF (ΔTime = $Time_{SBF}$ ± 1:00 hr.) at the M1 site.

Table S1. Aerosol radiative forcing in the atmosphere (ARF_{ATM}) estimated using the WRF-Chem model simulations at the M1 site.

Date	ARF_{ATM} Before SBF ($W\ m^{-2}$)	ARF_{ATM} After SBF ($W\ m^{-2}$)	Percentage change (After-Before)/Before x 100%
8-Jun	6.2	7.1	15.3
11-Jun	8.3	8.5	2.3
17-Jun	9.7	10.4	6.9
18-Jun	9.6	12.3	27.9
9-Jun	7.4	8.6	16.2
10-Jun	12.0	7.8	-34.8
12-Jun	11.6	10.7	-7.3
13-Jul	8.3	6.4	-22.9
16-Jul	8.0	7.0	-11.8
10-Aug	8.9	7.5	-16.3
11-Aug	19.7	12.0	-38.9